HHS Public Access

Author manuscript

Mol Immunol. Author manuscript; available in PMC 2021 February 01.

Published in final edited form as:

Mol Immunol. 2020 February ; 118: 110–116. doi:10.1016/j.molimm.2019.12.010.

Single-domain antibodies for functional targeting of the signaling scaffold Shoc2

Hyeln Jang, **Patricia G Wilson**, **Mary Sau**, **Udeep Chawla**, **David W Rodgers**, **Emilia Galperin**

Department of Molecular and Cellular Biochemistry, University of Kentucky, Lexington, KY 40536, United States.

Abstract

The accurate transmission of signals by the canonical ERK1/2 kinase pathway critically relies on the proper assembly of an intricate multiprotein complex by the scaffold protein Shoc2. However, the details of the mechanism by which Shoc2 guides ERK1/2 signals are not clear, in part, due to the lack of research tools targeting specific protein binding moieties of Shoc2. We report generation and characterization of single domain antibodies against human Shoc2 using a universal synthetic library of humanized nanobodies. Our results identify eight synthetic single-domain antibodies and show that two evaluated antibodies have binding affinities to Shoc2 in the nanomolar range. High affinity antibodies were uniquely suited for the analysis of the Shoc2 complex assembly. Selected single-domain antibodies were also functional in intracellular assays. This study illustrates that Shoc2 single-domain antibodies can be used to understand functional mechanisms governing complex multiprotein signaling modules and have promise in application for therapies that require modulation of the ERK1/2-associated diseases.

Keywords

Shoc2; single domain antibody; ERK1/2 signaling; scaffold

1. Introduction

Over the past two decades, single domain antibodies (sdAbs) have emerged as a valuable alternative to conventional antibodies and have found their applications in research as well as in therapeutics (Hassanzadeh-Ghassabeh, et al., 2013; Iezzi, et al., 2018; Lafaye and Li, 2018; Marschall and Dubel, 2016; Marschall, et al., 2016). Naturally found in sera of *Camelidae*, heavy chain only antibodies, also referred to as nanobodies or VHHs, are much

To whom correspondence should be addressed: Emilia Galperin, Department of Molecular and Cellular Biochemistry, University of Kentucky, 741 S Limestone Street, Lexington, KY 40536. Phone: 859-323-1796. Fax: 859-257-2283. emilia.galperin@uky.edu.

Author's contribution

HIJ designed and performed the experiments and drafted the manuscript; PW, MS and UC performed the experiments; DR designed the experiments; EG designed the experiments and wrote the manuscript.

Conflict of interest statement

The authors have no conflict of interest.

smaller in size than conventional antibodies (~15 kDa vs. ~150 kDa), and usually exhibit several superior properties compared to conventional antibodies in terms of enhanced solubility, low immunogenicity and stable folding in bacteria and the cytosol of eukaryotic cells (Muyldermans, 2001; Muyldermans, 2013). SdAb production usually includes preparation of the purified well-folded protein and immunization of camelids followed by relatively complex process selection and screening procedures (Beghein and Gettemans, 2017; Harmsen and De Haard, 2007). In this study, a fully synthetic phage display library of humanized llama single-domain antibodies was used to develop humanized synthetic sdAbs (hs2dAbs) against signaling scaffold Shoc2 (Moutel, et al., 2016).

The highly conserved scaffold protein Shoc2 regulates signal transduction of the canonical extracellular signal-regulated kinase (ERK1/2) pathway (Jang and Galperin, 2016). In the context of ERK1/2 signaling, the function of Shoc2 relies on its ability to engage various partners into a highly coordinated flow of interacting events (Jang, et al., 2015; Jang, et al., 2014; Jang, et al., 2019a; Rodriguez-Viciana, et al., 2006; Xie, et al., 2019; Young, et al., 2013). For example, Shoc2 scaffolds signaling proteins Ras and RAF-1 to accelerate growth-factor induced ERK1/2 activity (Matsunaga-Udagawa, et al., 2010; Rodriguez-Viciana, et al., 2006; Sieburth, et al., 1998). Shoc2 also nucleates a number of proteins of the ubiquitin machinery to fine-tune the ERK1/2 signals transduced through the module (Jang, et al., 2015; Jang, et al., 2014; Jang, et al., 2019a). Conventional approaches such as siRNA depletion, gene knock-down or overexpression of various functional mutants have been used to dissect the specific contributions of various Shoc2 partners in the molecular mechanisms regulating ERK1/2 signals (Jang, et al., 2015; Jang, et al., 2014; Jang, et al., 2019a; Rodriguez-Viciana, et al., 2006). However, biochemical tools that modulate the scaffolding abilities of Shoc2 allosterically or target specific protein-protein interacting interfaces directly have not been explored. Shoc2 interacts with several of its partners through non-overlapping interaction interfaces (Dai, et al., 2006; Jang, et al., 2015; Jang, et al., 2014; Jang, et al., 2019a; Rodriguez-Viciana, et al., 2006). For instance, Ras and RAF-1 proteins are recognized by the N-terminal domain of Shoc2, while the binding surfaces within the leucine-rich-repeats (LRR) domain are recognized by the E3 ligase HUWE1 and the AAA+ ATPases VCP and PSMC5 (Jang, et al., 2015; Jang, et al., 2014; Jang, et al., 2019a). Thus selective targeting of specific Shoc2 binding surfaces is likely to offer a unique handle on dissecting the fine modalities of the Shoc2-ERK1/2 signaling axis.

Signals transmitted via the Shoc2 scaffold module play a role in cancer biology and tumorigenesis (Jones, et al., 2019; Xie, et al., 2019). Missense mutations in the *shoc2* gene give rise to a developmental disorder with a wide spectrum of physiological and cognitive deficiencies, known as Noonan-like syndrome with loose anagen hair (NSLH) (Cordeddu, et al., 2009; Hannig, et al., 2014). Several studies have indicated that Shoc2 may have potential as a therapeutic target to modulate ERK1/2 signals (Jones, et al., 2019; Xie, et al., 2019). Thus, we envisioned that selective disruption of Shoc2 interactions with its binding partners or allosteric modulation of specific Shoc2 interactions can be utilized to influence the Shoc2-mediated ERK1/2 signals, and set out to generate and evaluate sdAbs targeting Shoc2.

In this study, we generated and characterized several Shoc2 hs2dAbs. We also established that selected hs2dAbs are valuable for fluorescence microscopy approaches and as an effective tool to study protein-protein interactions within the Shoc2 scaffold complex. Moreover, we found that when expressed in eukaryotic cells as intracellular antibodies (intrabodies), high affinity Shoc2 hs2dAbs altered the amplitude of the ERK1/2 phosphorylation. These results demonstrate the potential of Shoc2 hs2dAbs to selectively target the scaffolding complex and as a tool for development of treatments altering ERK1/2 signals.

2. Materials and Methods

2.1. Antibodies and other reagents

EGF was obtained from BD Biosciences. The following antibodies were used in this study: RFP (ThermoFisher Scientific), RAF-1, GAPDH, PSMC5, phospho-ERK1/2, and ERK1/2 (Santa Cruz Biotechnology); Shoc2 (Genetex), CP (BioLegend, San Diego, CA); HUWE1 (Bethyl, Montgomery, TX), Peroxidase-conjugated AffiniPure F(ab')2 Fragment Goat Anti-Rabbit and -Mouse IgG (H+L) (Jackson ImmunoResearch Laboratories, West Grove, PA). Anti-Scribble antibody was kindly provided by Dr. Tianyan Gao (University of Kentucky, Lexington, KY).

2.2. Library preparation and screening

Biotinylated Shoc2 was generated by Hybrigenics Services (http://www.hybrigenicsservices.com). Full-length human Shoc2 was cloned into the lexA vector pB27 as a LexAShoc2-C fusion and screened against the Nanobody Library Humanized 1 (NaLi-H1) library (Moutel, et al., 2016). Y2H screens were performed by Hybrigenics SA as described previously (Jang, et al., 2014).

2.3. Cloning, expression, cell culture and purification

293FT (Invitrogen, Carlsbad, CA, USA) and Cos1 cells (ATCC, Manassas, VA, USA) were grown in DMEM (Sigma, St. Louis, MO, USA) containing 10% FBS. The plasmids expressing Shoc2-tRFP, CFP-Rab7 and CFP-Rab5 were described previously (Galperin and Sorkin, 2003; Galperin and Sorkin, 2005). The transfection of DNA constructs was performed using PEI (Neo Transduction Laboratories, Lexington, KY, USA) reagents.

Fc-tagged hs2dAb fusion proteins were expressed in transiently transfected 293FT cells. Four to six days post-transfection, supernatants were harvested and cleared by centrifugation. hs2dAb-Fc fusion proteins were purified by affinity chromatography on protein G-sepharose (GE-Healthcare).

2.4. Immunoprecipitation and Western blot analysis

Cells were placed on ice and washed with Ca^{2+}, Mg^{2+}-free phosphate buffered saline (PBS), and the proteins were solubilized in 50 mM Tris (pH 7.5) containing 150 mM NaCl, 1% Triton X-100, 1 mM Na_3VO_4, 10 mM NaF, 0.5 mM phenylmethylsulfonyl fluoride (PMSF, Sigma, St. Louis, MO, USA), 10 μg/ml of leupeptin, and 10 μg/ml of aprotinin (Roche, Basel, Switzerland) for 15 min at 4°C. Lysates were then centrifuged at 14,000 rpm for 15

min to remove insoluble material. Lysates were incubated with appropriate antibodies for 2 hr, and the immunocomplexes were precipitated using protein A- or G-Sepharose (GE Healthcare Life Sciences, Chicago, IL, USA). Immunoprecipitates and aliquots of cell lysates were denatured in the sample buffer at 95°C, resolved by electrophoresis, and probed by Western blotting with various antibodies, followed by chemiluminescence detection.

Western blotting was done as described previously (Jeoung, et al., 2013). Proteins transferred from SDS-polyacrylamide gels to nitrocellulose membranes were visualized using a ChemiDoc analysis system (Bio-Rad, Hercules, CA, USA). Several exposures were analyzed to determine the linear range of the chemiluminescence signals. Quantification was performed using the densitometry analysis mode of Image Lab software (Bio-Rad, Hercules, CA, USA).

2.5. Immunofluorescence staining and analysis

Cells were grown on glass-bottom dishes and washed with Ca^{2+}, Mg^{2+}-free phosphate buffered saline (CMF-PBS). All images were acquired using a Mariannas Imaging system consisting of a Zeiss inverted microscope equipped with a cooled CCD CoolSnap HQ (Roper Technologies, Lakewood Ranch, FL, USA), dual filter wheels and a Lambda XL light source (Sutter Instruments, Novato, CA, USA), all controlled by SlideBook 6.0 software (Intelligent Imaging Innovations, Denver, CO, USA). Image analysis was performed using the SlideBook 6 software.

2.6. Biolayer Interferometry

The Shoc2-hs2dAb binding kinetics were determined using a ForteBio BLITZ instrument. Protein A Biosensors (Fortebio) were hydrated in buffer A (50 mM Tris-Cl (pH 7.4 @ 25°C), 300 mM NaCl, and 10 mM $MgCl_2$) for 50 min at room temperature. Sensors were then loaded with hs2dAb by incubating for about 1 min (hs2dAb concentration of 0.01mg/mL), followed by washing in buffer A for 30 s to remove unbound or weakly bound protein. BLITZ data readings were taken at 0.2 s intervals throughout these incubations. This was followed by incubating the hs2dAb-bound protein A biosensor with Shoc2 protein (0.03 mg/mL) for 2 minutes to determine Shoc2-hs2dAb association kinetics. Next the sensor was immersed in buffer A for 2 minutes to determine dissociation kinetics. A control for which Shoc2 was incubated with the protein-A biosensor (with no hs2dAb) was performed to rule out non-specific interaction of Shoc2 with protein A. Blitz data were imported into GraphPad Prism 8.0 and on and off rates, as well as dissociation constants, determined by nonlinear regression, fitting by least squares to the program's single-state association then dissociation equation. Association and dissociation data along with fitted curves were represented graphically with Prism 8.0.

2.7. Statistical analyses

Results are expressed as means ± SE. All statistical analyses were carried out using SigmaStat 13.0 (Systat Software Inc., Chicago, IL, USA)

3. Results

3.1. Selection of Shoc2-specific single-domain antibodies

To generate hs2dAb recognizing Shoc2, a phage display library coding for 3×10^9 hs2dAb clones was screened using biotinylated Shoc2(Moutel, et al., 2016). The initial round of screening yielded 5.13×10^5 clones that were then used to create a yeast two-hybrid (Y2H) library with the 1.19×10^6 cell complexity. The full length Shoc2 (NM_007373.2) was PCR-amplified and used as a bait in the following Y2H analysis (Fig. 1A). 3.2×10^6 interactions were tested yielding 190 positive clones with 8 different hs2dAbs sequences. All identified Shoc2 hs2dAbs contained four conserved framework regions and three variable complementarity determining regions (CDR). Amino acid sequence differences were observed within all three CDR regions, with the CDR3 region differing in length from 9 to 20 amino residues (Fig. 1B) (Moutel, et al., 2016). No clones contained cysteine residues in the CDR regions, thus disulfide bond formation within these regions is not a possibility. Differences in sequences of these clones suggested a potential diversity in epitopes.

3.2. Production and reformatting of single-domain antibodies

To expand their usability, recombinant hs2dAbs were then sub-cloned into a eukaryotic expression vector that carries the C-terminal chimeric rabbit-Fc-IgG2 and optimized for secretory protein production in HEK293 cells in serum free media. Western blot analysis of crude cell culture supernatants harvested 4 to 6 days after transfection revealed a prominent band at ~40 kDa corresponding to Shoc2 hs2dAbs (Fig. 2A). The secretion levels of Shoc2 hs2dAbs in cells varied considerably with hs2dAb^{B11}, hs2dAb^{B99} and hs2dAb^{B120} being secreted most efficiently. Secreted Shoc2-hs2dAbs often yielded double bands in SDS-PAGE analysis most likely as a consequence of proteolytic cleavage. Additionally, Shoc2 hs2dAbs were tagged with mCherry and expressed in Cos1 cells. Western blot analysis of cell lysates also showed some variability in expression of the mCherry-tagged Shoc2-hs2dAbs, indicating that intracellular environment possibly affects stability of hs2dAbs (Fig. 2B).

3.3. Determining the binding specificity and mapping of binding epitopes

In order to assess the immuno-reactivity of Shoc2-hs2dAbs, we analyzed whether they can precipitate Shoc2 protein in its native conformation. Data in Fig. 3A and B demonstrate that rFc-tagged hs2dAb^{B11}, hs2dAb^{B99} and hs2dAb^{B120} easily immuno-precipitated both an ectopically expressed Shoc2-tRFP as well as endogenous Shoc2 proteins, confirming the functionality of these hs2dAbs. rFc-tagged hs2dAb^{B28} and hs2dAb^{B189} immuno-precipitated Shoc2-tRFP in a less quantitative manner. rFc-tagged hs2dAb^{B11}, hs2dAb^{B99} and hs2dAb^{B120} immuno-precipitated endogenous Shoc2 as efficiently as the commercially-available polyclonal Shoc2 antibodies (Fig. 3A and B). None of the selected hs2dAbs recognized Shoc2 on Western blot, indicating that the Shoc2 hs2dAbs target conformational epitopes (*data not shown*).

We then chose hs2dAb^{B99} and hs2dAb^{B120} for further evaluation and determined the binding kinetics of hs2dAb^{B99} and hs2dAb^{B120} to Shoc2 using bio-layer interferometry. hs2dAb^{B99} and hs2dAb^{B120} were immobilized onto the biosensor, and then binding of

recombinant Shoc2 was monitored. We found that the affinity of hs2dAb^{B99} and hs2dAb^{B120} for Shoc2 is in nanomolar range, K_d values 14.4 nM (± 0.4) and 516 nM (±12) respectively, with hs2dAb^{B99} having a significantly tighter interaction (Fig. 3C and D).

In order to assess whether hs2dAb^{B99} and hs2dAb^{B120} recognize overlapping or distinct epitopes on Shoc2, a series of the previously validated Shoc2 deletion mutants was utilized (Fig. 3E) (Jeoung, et al., 2013). The interactions of hs2dAbs and Shoc2 were assessed by immunoprecipitation using lysates of Cos1 cells stably depleted of endogenous Shoc2 and transfected with either full-length or the truncated mutants of Shoc2-tRFP (Jang, et al., 2014) (Fig. 3F). We mapped the hs2dAb^{B99} and hs2dAb^{B120} recognition epitopes to the region connecting the unstructured N-terminal domain of Shoc2 with its C-terminal leucine rich repeats (LRR) domain (Fig. 3E and F). In addition, we established that hs2dAb^{B99} and hs2dAb^{B120} efficiently immuno-precipitated a number of known Shoc2 interacting partners (Fig. 3G), demonstrating that the high affinity Shoc2-hs2dAbs are a highly adaptive tool to study protein-protein interactions within the Shoc2 scaffolding complex.

3.4. Microscopy analysis of Shoc2 hs2dAb-mCherry intrabodies

A successful selection of single-domain antibodies using Y2H screening suggested that the hs2dAbs will be functional in the reducing environment of cytoplasm and can be used as intrabodies. In order to validate their functionality as intrabodies, we expressed individual hs2dAbs in HEK293 cells as mCherry-tagged constructs and examined their overall cellular distribution using live-cell fluorescence microscopy. Live fluorescence microscopy revealed that the cellular distribution of hs2dAb^{B97}, hs2dAb^{B120} and hs2dAb^{B99} resembled vesicular structures consistent with our earlier observations of Shoc2 translocating to endosomes (Galperin, et al., 2012; Jang, et al., 2015). We found that vesicles containing hs2dAb^{B97}, hs2dAb^{B99} and hs2dAb^{B120} were distributed throughout cells. The majority of the hs2dAb-labeled vesicles showed rapid movement, while some were relatively static and moved over short distances. To define the Shoc2-hs2dAb-containing vesicular compartments, Cos1 cells were transiently transfected with either CFP-Rab5 or CFP-Rab7, resident proteins of early and late endosomes, respectively. Shoc2-hs2dAbs were easily found on a population of CFP-Rab7-labeled late endosomes (Fig. 4A), but were not present on early endosomes labeled with CFP-Rab5. To further analyze the cellular distribution of hs2dAb^{B97}, hs2dAb^{B99} and hs2dAb^{B120}, we recruited Shoc2 to late endosomes/multivesicular bodies (LE/MVBs) by expressing oligomeric ATPase PSMC5 (GST-PSMC5) (Jang, et al., 2015). As shown in Fig. 4B, microscopy analysis of cells expressing GST-tagged PSMC5 and mCherry-tagged hs2dAb^{B97} revealed that hs2dAb^{B97} are recruited to the vesicular structures previously characterized as the late endosomal compartment(Jang, et al., 2015). Similar observations were made for hs2dAb^{B99} and hs2dAb^{B120} (*not shown*). Moreover, we found that mCherry-tagged hs2dAb^{B99} and hs2dAb^{B120} recognized the (S2G) mutant of Shoc2 that recruited to the plasma membrane due to aberrant myristoylation (Cordeddu, et al., 2009). Data in Fig. 4 support the notion that Shoc2 hs2dAb can be used for a number of intracellular assays.

3.5. The effect of anti-Shoc2 nanobodies on ERK1/2 activation

In order to evaluate whether Shoc2 hs2dAbs alter the Shoc2-mediated intracellular ERK1/2 signals, we overexpressed individual mCherry-tagged hs2dAbs and examined ERK1/2

phosphorylation (pERK1/2). We found that in cells expressing hs2dAb^{B11}, hs2dAb^{B18}, hs2dAb^{B28}, hs2dAb^{B97}, hs2dAb^{B98} or hs2dAb^{B189} and treated with epidermal growth factor (EGF) levels of pERK1/2 were not affected (Fig. 5A). The expression of Shoc2-hs2dAbs was validated by fluorescence microscopy (*not shown*). However, in cells expressing mCherry-tagged hs2dAb^{B99} and hs2dAb^{B120} amplitude of pERK1/2 was markedly increased (Fig. 5B). We then determined whether the expression of hs2dAb^{B99} affects ERK1/2 phosphorylation in cells carrying the Shoc2-S2G mutant (Galperin, et al., 2012). Cos1 cells stably expressing the Shoc2–tRFP (S2G) mutant and depleted of endogenous Shoc2 (Shoc2-S2G-tR) were transfected with mCherry-tagged hs2dAb^{B99} (Fig. 5B). The expression of hs2dAb^{B99} partially restored the amplitude of the EGF-induced ERK1/2 phosphorylation in cells expressing Shoc2-S2G-tR, further indicating that hs2dAb^{B99} modulate signal transmission *via* the Shoc2 signaling complex. Together, these results strongly suggest that hs2dAb^{B99} and hs2dAb^{B120} facilitate Shoc2-mediated ERK1/2 activation.

4. Discussion/Conclusion

The role of the Shoc2 scaffold protein in regulating specificity of ERK1/2 signals has been well-recognized by a number of studies (Boned Del Rio, et al., 2019; Jang, et al., 2019b; Jeoung, et al., 2016; Li, et al., 2000; Rauen, 2013; Rodriguez-Viciana, et al., 2006). Shoc2 assembles intricate multi-protein complex machinery that accelerates and fine-tunes the amplitude of ERK1/2 signals (Jang and Galperin, 2016). However, advanced methodologies are needed to fully appreciate the multifaceted feedback mechanisms modulating the ERK1/2 signals *via* the Shoc2/Ras/RAF-1 complex. The goal of the present study was to produce functional Shoc2-hs2dAbs that target specific Shoc2 interfaces and modify Shoc2-ERK1/2 signaling outcomes.

The technology of cloning the antigen-binding fragments from an immunized animal into phage display vector following selection of the antigen-specific clones is well-established and has become a routine method to identify antigen specificity. Yet, immunization is a time-consuming process that requires the costly maintenance of large animals (Harmsen and De Haard, 2007). Recent advances in development of synthetic VHH libraries allow avoiding animal immunization altogether. Although synthetic libraries have advantage of expanded repertoires, they lack the benefit of affinity maturation and rarely produce high affinity monovalent binders (Ingram, et al., 2018). In this study, we used a synthetic library that is based on a non-immune humanized VHH scaffold optimized for stability and ease of expression and was previously utilized for the successful selection of conformation-specific high affinity sdAbs (Moutel, et al., 2016). Selection and generation of functional hs2dAbs directed against the scaffold protein Shoc2 was possible without a common requirement for large amounts of recombinant Shoc2 protein or animal immunization (Fig. 1–3). Several functional hs2dAbs against Shoc2 were successfully selected using conventional Y2H screening. The selected hs2dAbs were expressed, purified and verified for specificity against Shoc2. To the best of our knowledge, these are the first reported single domain high-affinity antibodies against Shoc2. These Shoc2-hs2dAbs are stable intracellularly and several of the selected hs2dAbs are suitable for functional essays using microscopy approaches as intrabodies (Fig. 4).

Intrabodies have been used to visualize endogenous proteins using microscopy (Beghein and Gettemans, 2017). But, the most appealing application is to use intrabodies to explore protein function and, if possible, rapid protein inactivation in living cells (Beghein and Gettemans, 2017; Marschall and Dubel, 2016; Marschall, et al., 2015). Thus, our intrabodies were evaluated for the possibility of disturbing Shoc2-ERK1/2 signaling. Unexpectedly, we observed that in cells expressing high affinity hs2dAb^{99} and hs2dAb^{120} we consistently detected an increase in phospho-ERK1/2 (Fig. 5). The binding regions of hs2dAb^{99} and hs2dAb^{120} was mapped to the hinge region between the N-terminus and LRR domain of Shoc2 (Fig. 3). Thus, it is possible that this region of Shoc2 is recognized by the unknown Shoc2 binder that supports interaction of the signaling partner in the complex, Ras and Raf-1. Alternatively, sdAbs binding to Shoc2 may prevent binding of the unknown negative regulator in the Shoc2 complex and/or hs2dAb binding can interfere with deactivating changes in Shoc2 protein folding that occur upon stimulation of the ERK1/2 pathway. These scenarios, however, require further studies using methodologies that will identify additional components of the Shoc2 complex. Equally interesting are our findings that in cells carrying the Shoc2-S2G-tRFP mutant, hs2dAb^{99} have partially rescued ERK1/2 phosphorylation. These results suggest that Shoc2 hs2dAbs may potentially be explored as therapeutic agents.

In conclusion, results of this study establish novel tools to analyze regulation of the canonical ERK1/2 signaling pathway. We report for the first time production of the Shoc2 specific hs2dAb using a synthetic library. The Shoc2 hs2dAb developed in this study are stable, high affinity and should be considered for further studies evaluating and clarifying the pathophysiological significance of the multiple protein-protein interactions within the Shoc2 complex.

Acknowledgements

We thank Dr. Craig Vander Kooi for critical reading of the manuscript and Dr. Tianyan Gao for sharing valuable reagents. This project was supported by grants from the National Institute of General Medical Sciences (GM113087 to EG) and the American Cancer Society (RSG-14-172-01-CSM to EG). Its content is solely the responsibility of the authors and does not necessarily represent the official views of the National Institute of Health.

References

Beghein E, Gettemans J. 2017 Nanobody Technology: A Versatile Toolkit for Microscopic Imaging, Protein-Protein Interaction Analysis, and Protein Function Exploration. Front Immunol 8:771. [PubMed: 28725224]

Boned Del Rio I, Young LC, Sari S, Jones GG, Ringham-Terry B, Hartig N, Rejnowicz E, Lei W, Bhamra A, Surinova S, Rodriguez-Viciana P. 2019 SHOC2 complex-driven RAF dimerization selectively contributes to ERK pathway dynamics. Proc Natl Acad Sci U S A 116(27):13330–13339. [PubMed: 31213532]

Cordeddu V, Di Schiavi E, Pennacchio LA, Ma'ayan A, Sarkozy A, Fodale V, Cecchetti S, Cardinale A, Martin J, Schackwitz W, Lipzen A, Zampino G, et al. 2009 Mutation of SHOC2 promotes aberrant protein N-myristoylation and causes Noonan-like syndrome with loose anagen hair. Nature genetics 41(9):1022–6. [PubMed: 19684605]

Dai P, Xiong WC, Mei L. 2006 Erbin inhibits RAF activation by disrupting the sur-8-Ras-Raf complex. The Journal of biological chemistry 281(2):927–33. [PubMed: 16301319]

Galperin E, Abdelmoti L, Sorkin A. 2012 Shoc2 is targeted to late endosomes and required for Erk1/2 activation in EGF-stimulated cells. PLoS One 7(5):e36469. [PubMed: 22606262]

Galperin E, Sorkin A. 2003 Visualization of Rab5 activity in living cells by FRET microscopy and influence of plasma-membrane-targeted Rab5 on clathrin-dependent endocytosis. Journal of cell science 116(Pt 23):4799–810. [PubMed: 14600265]

Galperin E, Sorkin A. 2005 Visualization of Rab5 activity in living cells using FRET microscopy. Methods in enzymology 403:119–34. [PubMed: 16473582]

Hannig V, Jeoung M, Jang ER, Phillips JA 3rd, Galperin E. 2014 A Novel SHOC2 Variant in Rasopathy.

Hum Mutat. Harmsen MM, De Haard HJ. 2007 Properties, production, and applications of camelid single-domain antibody fragments. Appl Microbiol Biotechnol 77(1):13–22. [PubMed: 17704915]

Hassanzadeh-Ghassabeh G, Devoogdt N, De Pauw P, Vincke C, Muyldermans S. 2013 Nanobodies and their potential applications. Nanomedicine (Lond) 8(6):1013–26. [PubMed: 23730699]

Iezzi ME, Policastro L, Werbajh S, Podhajcer O, Canziani GA. 2018 Single-Domain Antibodies and the Promise of Modular Targeting in Cancer Imaging and Treatment. Front Immunol 9:273. [PubMed: 29520274]

Ingram JR, Schmidt FI, Ploegh HL. 2018 Exploiting Nanobodies' Singular Traits. Annu Rev Immunol 36:695–715. [PubMed: 29490163]

Jang ER, Galperin E. 2016 The function of Shoc2: A scaffold and beyond. Commun Integr Biol 9(4):e1188241. [PubMed: 27574535]

Jang ER, Jang H, Shi P, Popa G, Jeoung M, Galperin E. 2015 Spatial control of Shoc2-scaffold-mediated ERK1/2 signaling requires remodeling activity of the ATPase PSMC5. J Cell Sci 128(23):4428–41. [PubMed: 26519477]

Jang ER, Shi P, Bryant J, Chen J, Dukhante V, Gentry MS, Jang H, Jeoung M, Galperin E. 2014 HUWE1 is a molecular link controlling RAF-1 activity supported by the Shoc2 scaffold. Mol Cell Biol.

Jang H, Jang ER, Wilson PG, Anderson D, Galperin E. 2019a VCP/p97 controls signals of the ERK1/2 pathway transmitted via the Shoc2 scaffolding complex: novel insights into IBMPFD pathology. Mol Biol Cell:mbcE19030144.

Jang H, Oakley E, Forbes-Osborne M, Kesler MV, Norcross R, Morris AC, Galperin E. 2019b Hematopoietic and neural crest defects in zebrafish shoc2 mutants: a novel vertebrate model for Noonan-like syndrome. Hum Mol Genet 28(3):501–514. [PubMed: 30329053]

Jeoung M, Abdelmoti L, Jang ER, Vander Kooi CW, Galperin E. 2013 Functional Integration of the Conserved Domains of Shoc2 Scaffold. PLoS One 8(6):e66067. [PubMed: 23805200]

Jeoung M, Jang ER, Liu J, Wang C, Rouchka EC, Li X, Galperin E. 2016 Shoc2-tranduced ERK1/2 motility signals--Novel insights from functional genomics. Cell Signal 28(5):448–459. [PubMed: 26876614]

Jones GG, Del Rio IB, Sari S, Sekerim A, Young LC, Hartig N, Areso Zubiaur I, El-Bahrawy MA, Hynds RE, Lei W, Molina-Arcas M, Downward J, et al. 2019 SHOC2 phosphatase-dependent RAF dimerization mediates resistance to MEK inhibition in RAS-mutant cancers. Nat Commun 10(1):2532. [PubMed: 31182717]

Lafaye P, Li T. 2018 Use of camel single-domain antibodies for the diagnosis and treatment of zoonotic diseases. Comp Immunol Microbiol Infect Dis 60:17–22. [PubMed: 30396425]

Li W, Han M, Guan KL. 2000 The leucine-rich repeat protein SUR-8 enhances MAP kinase activation and forms a complex with Ras and Raf. Genes & development 14(8):895–900. [PubMed: 10783161]

Marschall AL, Dubel S. 2016 Antibodies inside of a cell can change its outside: Can intrabodies provide a new therapeutic paradigm? Comput Struct Biotechnol J 14:304–8. [PubMed: 27570612]

Marschall AL, Dubel S, Boldicke T. 2015 Specific in vivo knockdown of protein function by intrabodies. MAbs 7(6):1010–35. [PubMed: 26252565]

Marschall AL, Dubel S, Boldicke T. 2016 Recent Advances with ER Targeted Intrabodies. Adv Exp Med Biol 917:77–93. [PubMed: 27236553]

Matsunaga-Udagawa R, Fujita Y, Yoshiki S, Terai K, Kamioka Y, Kiyokawa E, Yugi K, Aoki K, Matsuda M. 2010 The scaffold protein Shoc2/SUR-8 accelerates the interaction of Ras and Raf. J Biol Chem 285(10):7818–26. [PubMed: 20051520]

Moutel S, Bery N, Bernard V, Keller L, Lemesre E, de Marco A, Ligat L, Rain JC, Favre G, Olichon A, Perez F. 2016 NaLi-H1: A universal synthetic library of humanized nanobodies providing highly functional antibodies and intrabodies. Elife 5.

Muyldermans S 2001 Single domain camel antibodies: current status. J Biotechnol 74(4):277–302. [PubMed: 11526908]

Muyldermans S 2013 Nanobodies: natural single-domain antibodies. Annu Rev Biochem 82:775–97. [PubMed: 23495938]

Rauen KA. 2013 The RASopathies. Annu Rev Genomics Hum Genet.

Rodriguez-Viciana P, Oses-Prieto J, Burlingame A, Fried M, McCormick F. 2006 A phosphatase holoenzyme comprised of Shoc2/Sur8 and the catalytic subunit of PP1 functions as an M-Ras effector to modulate Raf activity. Mol Cell 22(2):217–30. [PubMed: 16630891]

Sieburth DS, Sun Q, Han M. 1998 SUR-8, a conserved Ras-binding protein with leucine-rich repeats, positively regulates Ras-mediated signaling in C. elegans. Cell 94(1):119–30. [PubMed: 9674433]

Xie CM, Tan M, Lin XT, Wu D, Jiang Y, Tan Y, Li H, Ma Y, Xiong X, Sun Y. 2019 The FBXW7-SHOC2-Raptor Axis Controls the Cross-Talks between the RAS-ERK and mTORC1 Signaling Pathways. Cell Rep 26(11):3037–3050 e4. [PubMed: 30865892]

Young LC, Hartig N, Munoz-Alegre M, Oses-Prieto JA, Durdu S, Bender S, Vijayakumar V, Vietri Rudan M, Gewinner C, Henderson S, Jathoul AP, Ghatrora R, et al. 2013 An MRAS, SHOC2, and SCRIB Complex Coordinates ERK Pathway Activation with Polarity and Tumorigenic Growth. Mol Cell 52(5):679–92. [PubMed: 24211266]

Highlights

- Eight single-domain antibodies (sdAbs) targeting Shoc2 were selected from the synthetic phage display library of humanized llama sdAbs.
- sdAbs were purified and examined for immunoreactivity and intracellular reactivity.
- High affinity Shoc2 sdAbs can efficiently precipitate a number of proteins in the scaffolding complex.
- Selected Shoc2 sdAbs affect ERK1/2 signals when expressed intracellularly.

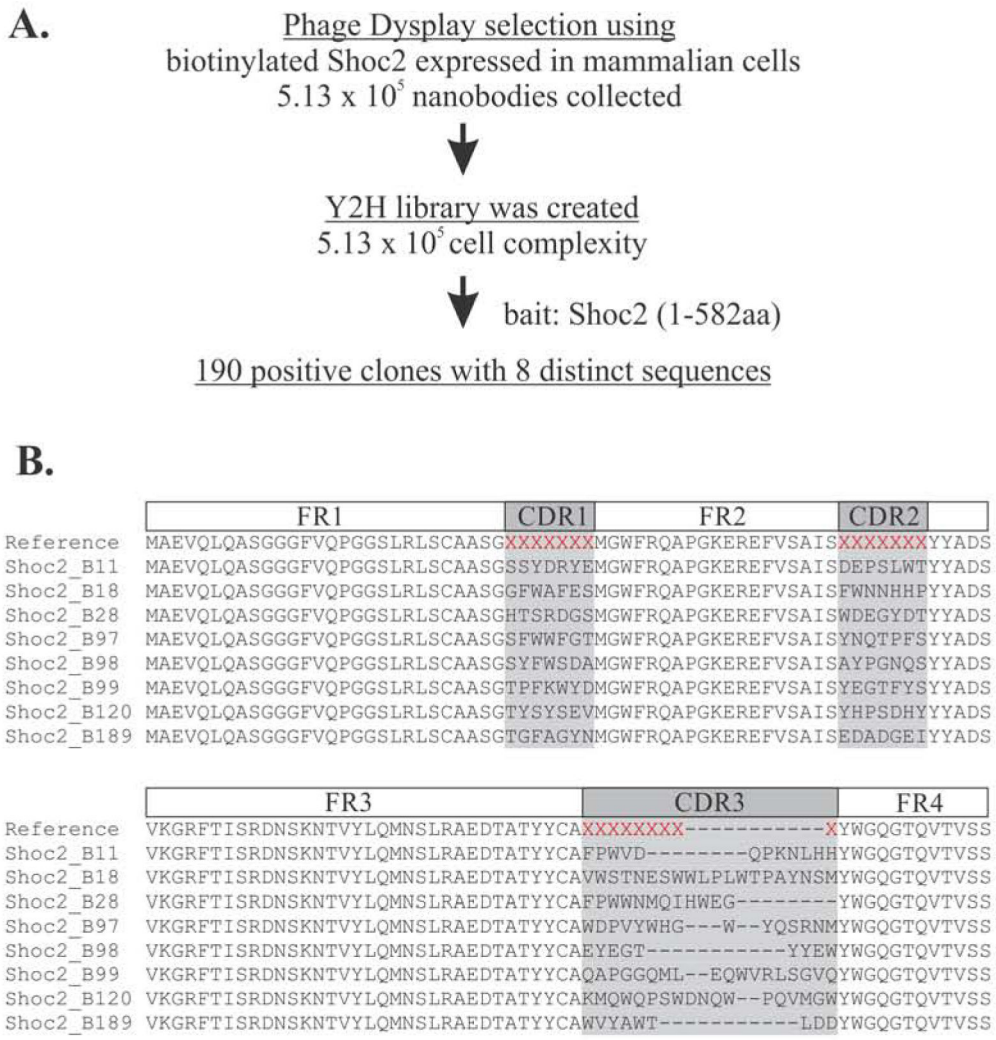

Figure 1. Selection of single-domain antibody

(A) Diagram summarizing the experimental flow of using humanized synthetic single domain antibody library (hs2dAb) to select Shoc2 antibody.

(B) Amino acid sequence of 8 different anti-Shoc2 hs2dAbs. FR- Frame work, CDR- Complementarity Determining Regions

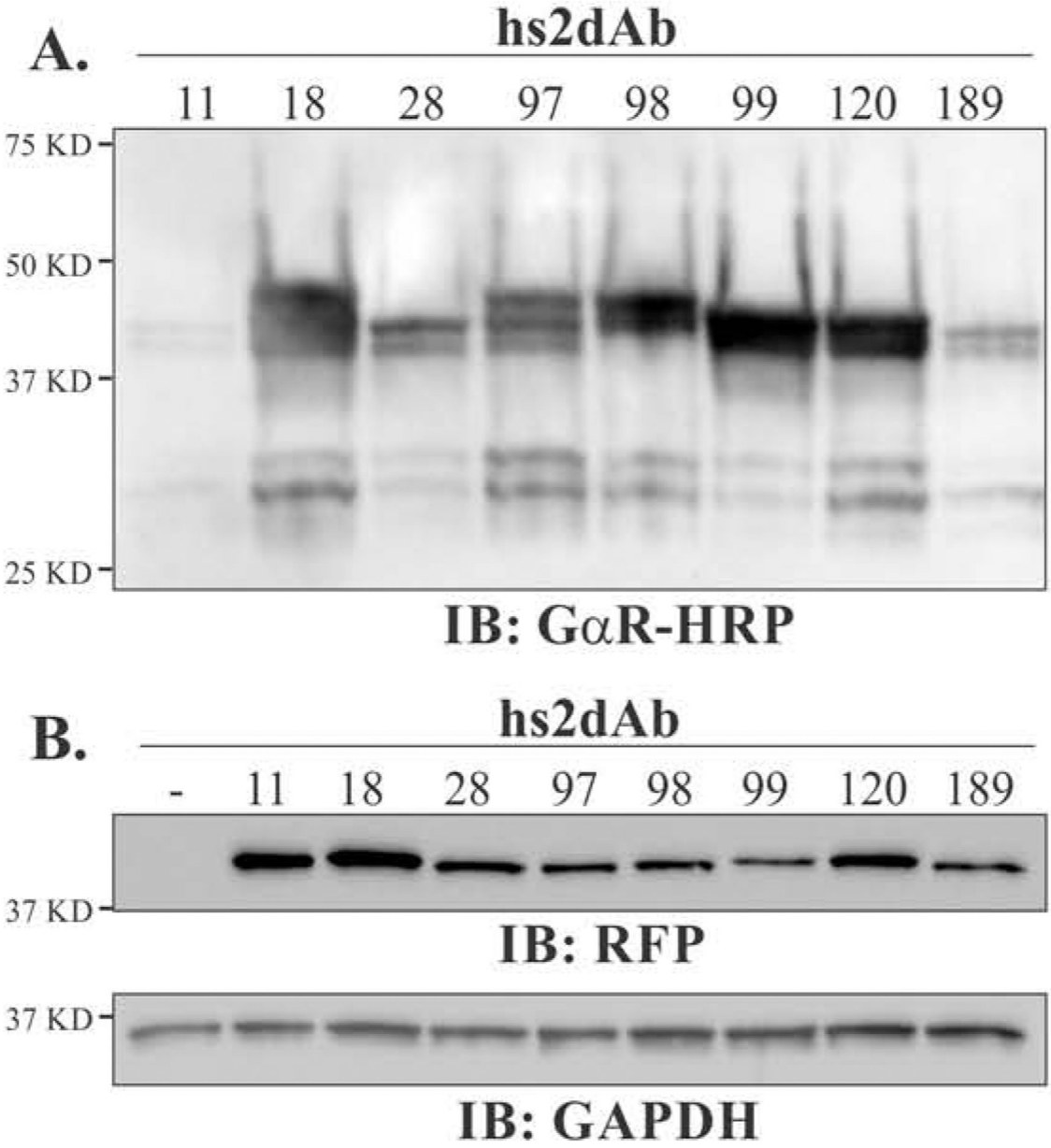

Figure 2. Expression of Shoc2 hsd2Abs

(A) 293FT cells were transfected with different Fc-tagged Shoc2-hs2dAbs. Cell media was analyzed four days post-transfection by immunoblotting using anti-rabbit antibodies.

(B) mCherry-tagged Shoc2-hsd2Abs were expressed in Cos1 cells. Shoc2-hs2dAbs were detected in cell lysates by immunoblotting using anti-RFP antibodies. The results in each panel are representative of three independent experiments.

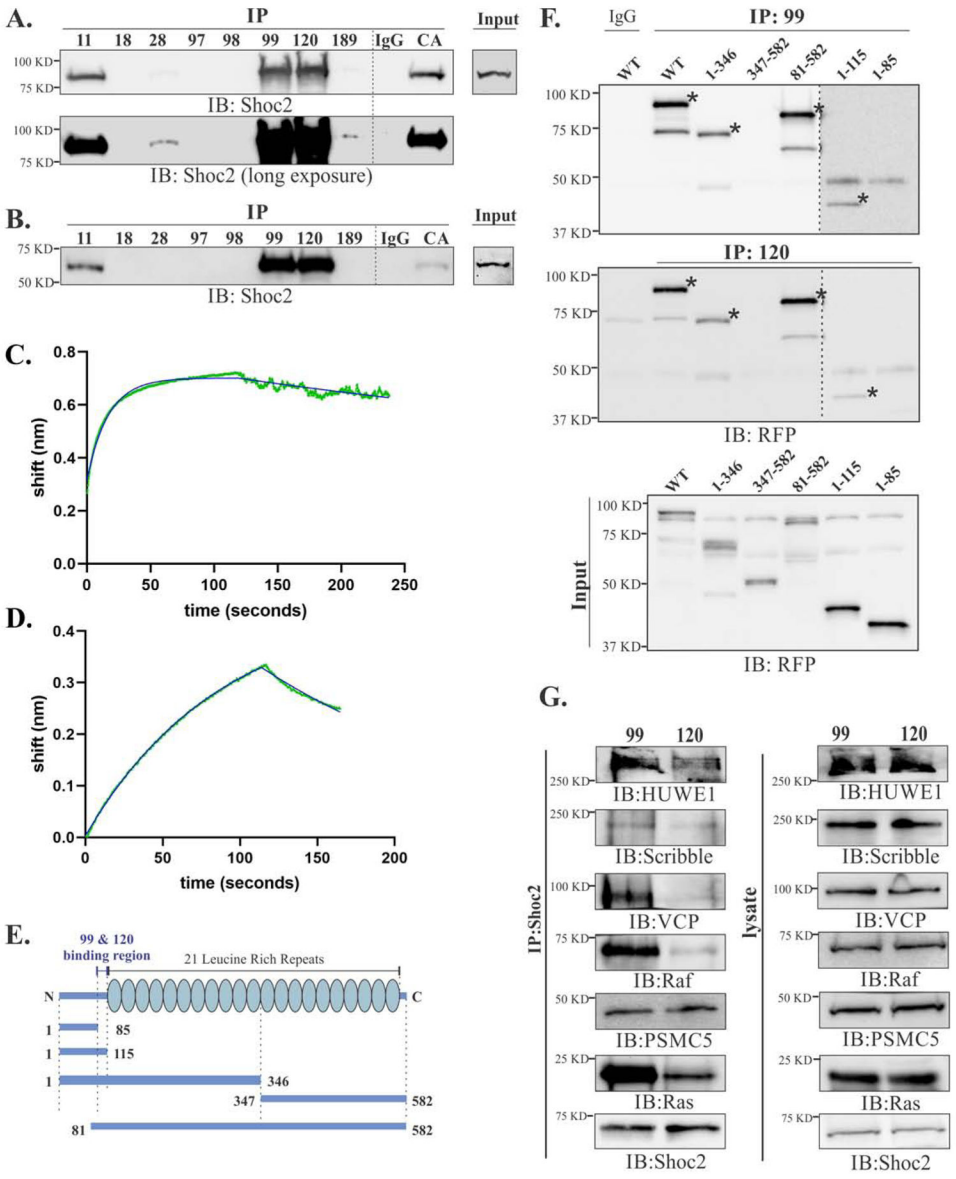

Figure 3. Mapping the Shoc2 hsd2Abs epitopes

(A) YFP-tagged Shoc2 was immunoprecipitated from Cos1 cells depleted of endogenous Shoc2 and stably expressing YFP-tagged Shoc2 using either anti-Shoc2 hs2dAbs or commercially available (CA) anti-Shoc2 antibody. Shoc2 was detected in immunoprecipitates using anti-Shoc2 antibodies.

(B) Endogenous Shoc2 was immunoprecipitated from Cos1 cells using either Shoc2-hs2dAbs or commercially available (CA) anti-Shoc2 antibody. Shoc2 was detected in immunoprecipitates using anti-Shoc2 antibodies. The results in each panel are representative of those from three independent experiments.

(C-D) Biolayer interferometry analysis of Shoc2 binding to Shoc2-hs2dAbs. Shown are raw data (green) and best-fit lines of Shoc2 binding to (C) hs2dAb^{99} or (D) hs2dAb^{120}. (E) Schematic representation of the Shoc2 truncated mutants used in the experiments presented in panel D.

(F) Cos1 cells constitutively depleted of Shoc2 were co-transfected with the Shoc2-tRFP truncated mutants depicted in panel C. Shoc2 was immunoprecipitated and analyzed by immunoblotting using anti-tRFP antibodies.
(G) Shoc2 was immunoprecipitated from 293FT cells. Shoc2 and its interacting partners were detected in immunoprecipitates by Western blotting using specific antibodies.

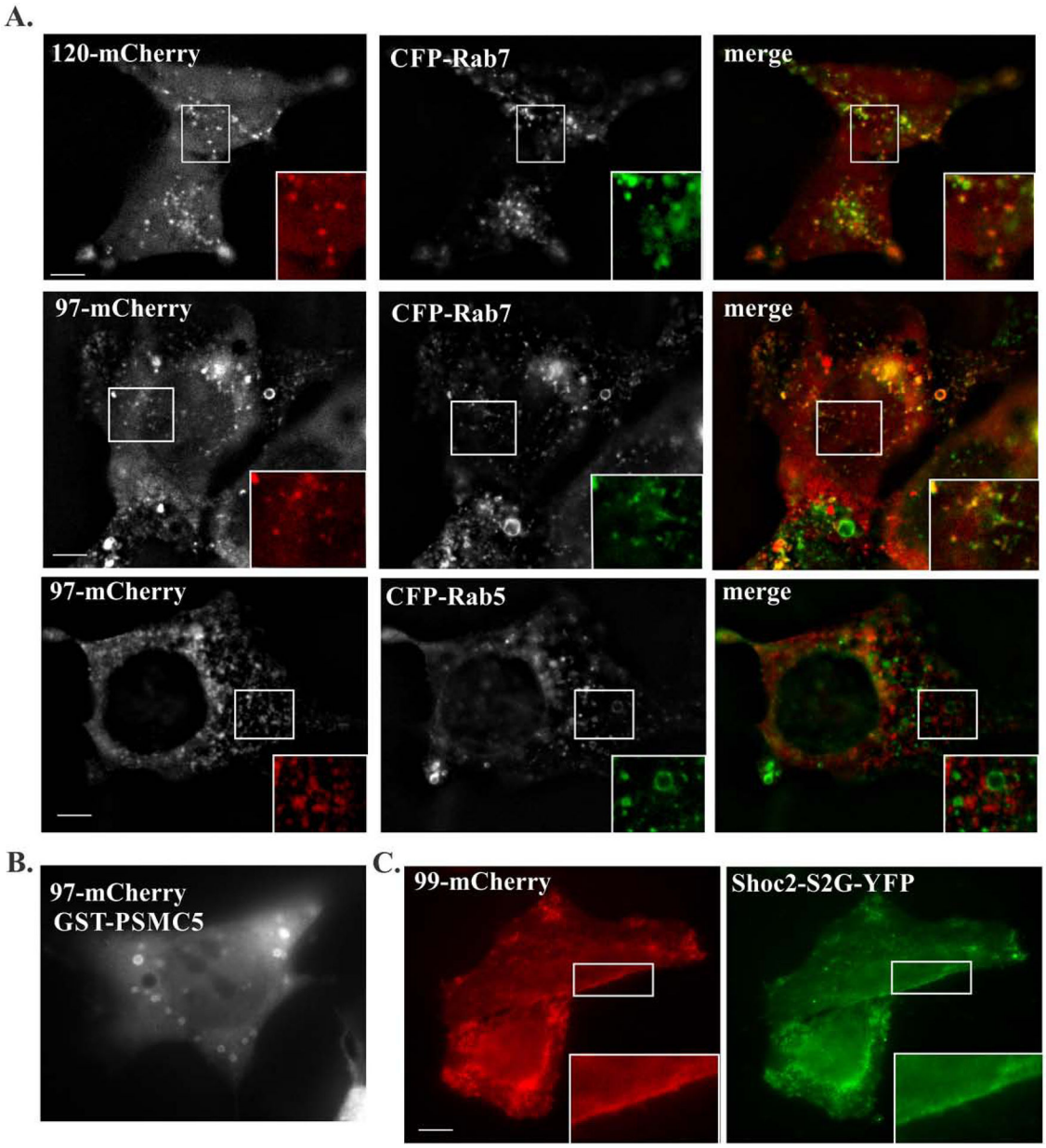

Figure 4. Intracellular analysis of Shoc2-hsd2Abs

(A) Cos-SR cells expressing hs2dAb^{120} or hs2dAb^{97} and CFP-Rab5 or CFP-Rab7 were followed by immunofluorescence microscopy. Insets show high magnification images of the region indicated by white rectangles. Scale bars: 10 μm.

(B) Cos1 cells were transfected with GST-PSMC5 and mCherry-tagged hs2dAb^{97}. Cells were followed by immunofluorescence microscopy. Insets show high magnification images of the regions of the cell indicated by white rectangles. Scale bars: 10 μm.

(C) Cos1 cells were transfected with Shoc2 (S2G)-YFP and hs2dAb^{99}. Cells were followed by immunofluorescence microscopy. Insets show high magnification images of the regions of the cell indicated by white rectangles. Scale bars: 10 μm.

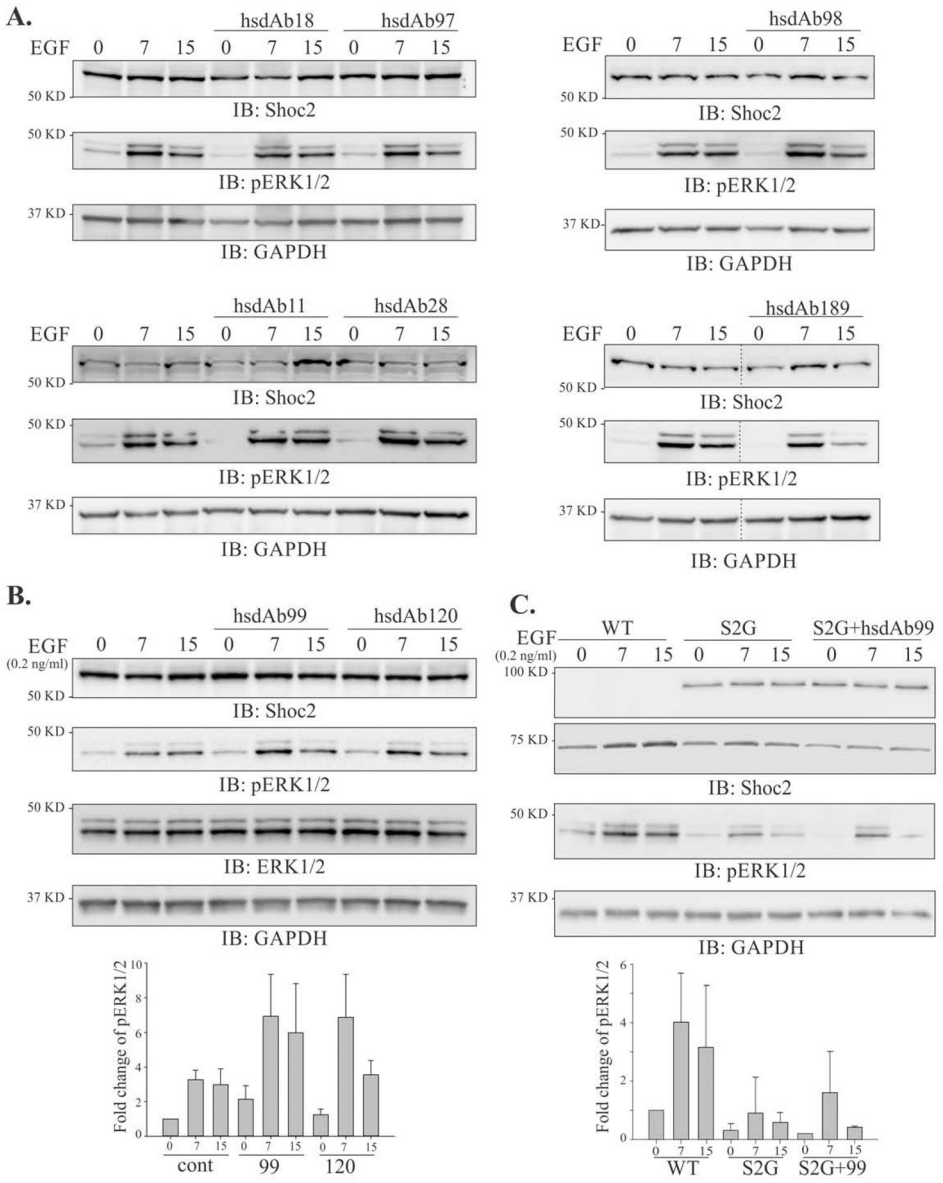

Figure 5. Effect of Shoc2-hsd2Abs on ERK1/2 phosphorylation

(A and B) Cos1 cells transfected with different hs2dAbs were serum-starved for 16 hr and then stimulated with EGF (0.2 ng/ml) for 7 and 15 min. Immunoblots were analyzed with anti-Shoc2, -GAPDH, -ERK1/2 and -pERK1/2 antibodies. The results in each panel are representative of three independent experiments. Blots from the multiple experiments in B were analyzed. Bars represent the mean ± S.E. (n=3) for pERK1/2 normalized to the value for GAPDH in arbitrary units (p<0.01, by Student's t-test). The results in each panel are representative of three independent experiments.

(C) Cos1 cells transfected with Shoc2 (S2G)-YFP and hs2dAb^{99} were serum-starved for 16 hr and then stimulated with EGF (0.2 ng/ml) for 7 and 15 min. Immunoblots were analyzed with anti-Shoc2, -GAPDH, and -pERK1/2 antibodies. The results in each panel are representative of three independent experiments.